

# Probability Estimation for Predicted-Occupancy Grids in Vehicle Safety Applications Based on Machine Learning

Parthasarathy Nadarajan<sup>1</sup> and Michael Botsch<sup>1</sup>

**Abstract**—This paper presents a method to predict the evolution of a complex traffic scenario with multiple objects. The current state of the scenario is assumed to be known from sensors and the prediction is taking into account various hypotheses about the behavior of traffic participants. This way, the uncertainties regarding the behavior of traffic participants can be modelled in detail. In the first part of this paper a model-based approach is presented to compute *Predicted-Occupancy Grids* (POG), which are introduced as a grid-based probabilistic representation of the future scenario hypotheses. However, due to the large number of possible trajectories for each traffic participant, the model-based approach comes with a very high computational load. Thus, a machine-learning approach is adopted for the computation of POGs. This work uses a novel grid-based representation of the current state of the traffic scenario and performs the mapping to POGs. This representation consists of augmented cells in an occupancy grid. The adopted machine-learning approach is based on the Random Forest algorithm. Simulations of traffic scenarios are performed to compare the machine-learning with the model-based approach. The results are promising and could enable the real-time computation of POGs for vehicle safety applications. With this detailed modelling of uncertainties, crucial components in vehicle safety systems like criticality estimation and trajectory planning can be improved.

## I. INTRODUCTION

In recent years the field of Active Vehicle Safety gained significant importance due to the availability of sensors like radar, cameras, laserscanners, etc. Using the information of such exteroceptive sensors, vehicles are capable of estimating the criticality of traffic scenarios and to avoid or mitigate collisions. For example, the Autonomous Emergency Braking [1] is an important Active Vehicle Safety system that is already available on the market. One of the major challenges for Active Vehicle Safety systems is the prediction on how a traffic scenario can evolve in a given time horizon. Predictions over a short interval of time, which for most safety applications is less than approx. 1 s, can be estimated based on the current state of the traffic objects [2]. These states contain physical quantities like velocities, yaw rates, accelerations etc. However, predictions over longer horizons

© 2016 IEEE. Personal use of this material is permitted. Permission from IEEE must be obtained for all other uses, in any current or future media, including reprinting/republishing this material for advertising or promotional purposes, creating new collective works, for resale or redistribution to servers or lists, or reuse of any copyrighted component of this work in other works. This is the author's accepted manuscript version of the paper: "Probability estimation for Predicted-Occupancy Grids in vehicle safety applications based on machine learning" by P. Nadarajan and M. Botsch, published in the 2016 IEEE Intelligent Vehicles Symposium (IV), Gothenburg, Sweden, pp. 1285–1292, 2016. DOI: 10.1109/IVS.2016.7535556.

<sup>1</sup>Technische Hochschule Ingolstadt, Esplanade 10 Ingolstadt, Germany

depend largely on the interaction and the motivation of the traffic participants in a particular traffic scene.

In recent years several contributions were made in anticipating the behavior of traffic participants by incorporating the intention of the driver and the interaction between the participants. For longer periods of prediction, the methods can be categorized into pattern recognition in motion pattern databases [3], [4] and methods which fuse dynamic motion models with behavior and environment description [5]. There are also a number of approaches which predict the evolution of a traffic scene on a more abstract level. The models consist of probabilistic state machines [6], static Bayesian Networks [7], dynamic Bayesian Networks [8], Hidden Markov Models [9] or fuzzy-theory [6]. In [10], long-term trajectory prediction is based on a combination of high-level Bayesian maneuver detection with imminent uncertainty of maneuver execution by drivers. In [11] and [12], a dynamic Bayesian Network is used to model the interaction between an arbitrary number of traffic participants.

In order to make accurate predictions, the representation of the environment plays an important role. The objects in the environment vary a lot with respect to their geometries and description of these objects can be quite complex. One of the established methods to overcome this problem is the occupancy grid framework [13]. The occupancy grid divides the environment into a grid of cells and the occupancy of each of the cells being occupied or empty is estimated. Occupancy grids find their application in sensor data fusion [14], path planning [15], simultaneous localization and mapping (SLAM) [16] and target tracking [17]. Work also has been done for the representation of dynamic situations with occupancy grids. The basic Bayesian occupancy filter combines the occupancy grid representation of static environments with probabilistic velocity objects to build a dynamic map of the environment. In [17], a different formulation with a 2-D occupancy, where each cell has an associated distribution over its possible velocities is adopted.

In this paper, a novel method for the representation and prediction of traffic scenes using occupancy grids is formulated. The main idea is to augment the cells with information about the infrastructure and traffic participants, e.g., acceleration, velocity and yaw angle, and then to use this representation for predictions. The result is called *Predicted-Occupancy Grid* (POG) and includes the uncertainty about the future motion of traffic objects. Due to the high computational complexity necessary to model and evaluate a large number of motion hypotheses for each object, the approach introduced in this work to enable real-time computation is

based on machine learning. The evolution of a traffic scenario is estimated as a Predicted-Occupancy grid using the *Random Forest* (RF) algorithm [18].

The outline of the paper is as follows. Section II introduces the concept of POGs. Section III deals with the machine learning technique used for the probability estimation for POGs. The evaluation of the machine-learning approach with simulation results is presented in Section IV. The applications of the current approach towards the field of Vehicle Safety is discussed in Section V.

Throughout this work, vectors and matrices are denoted by lower and upper case bold letters, and random variables are written using sans serif fonts. A lower-case bold letter represents a column vector.

## II. PREDICTED-OCCUPANCY GRIDS

In II-A and II-B, the theoretical background for the development of a model-based approach for the computation of POG is presented. The models will also be used for the generation of a training data set for the machine-learning approach.

### A. Dynamic Models of Traffic Objects

To construct POGs, a fundamental task is the motion-prediction of objects in traffic scenarios. This prediction requires dynamic models which are used to compute future trajectories. In [19] a survey on dynamic vehicle models and their performance for tracking tasks are presented. For tracking tasks, simple linear models like the Constant Velocity (CV) or Constant Acceleration (CA) models can be used. But for a better performance, curvilinear models like Constant Turn Rate and Velocity (CTRV), Constant Turn Rate and Acceleration (CTRA), Constant Steering Angle and Velocity (CSAV), or Constant Curvature and Acceleration (CCA) are used.

Since the focus in this paper is to predict the planar motion of objects in traffic scenarios with high accuracy, more sophisticated models than the ones presented in [19] are used. The CV, CA, CTRV, CTRA, CSAV, and CCA models are simplifications of the single-track vehicle model, that is often called bicycle model. The single-track model is a simplification of the two-track model which is presented in the following.

1) *Two-Track Model*: The planar motion of 4-wheel cars can be described accurately using a two-track model. It is a nonlinear planar vehicle dynamic model which describes the vehicle as a rigid body and models the forces that act on the 4 tires. Fig. 1 shows the planar view of a vehicle and presents the quantities that are needed to derive the two-track model starting from the balance of forces and moments. The vehicle coordinate system has the unit vectors  $e_x$ ,  $e_y$ , and  $e_z$ . The center of gravity is denoted with  $C$ , the track width with  $w$ , the wheel-base with  $\ell$ , the slip angle with  $\beta$ , the velocity vector with  $v$ , the yaw-rate with  $\dot{\psi}$ , and the steering angles at each wheel with  $\delta_i$ , where the subscript  $i \in \{\text{fl, fr, rl, rr}\}$  indicates whether it is the front left (fl), front right (fr), rear left (rl) or rear right (rr) wheel. The same subscript notation

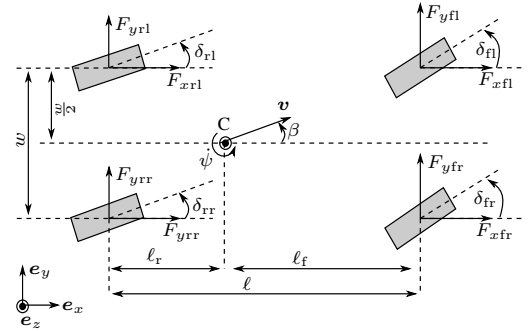


Fig. 1. Two-track model

is used for the forces  $F_{xi}$  and  $F_{yi}$  acting on each wheel. Denoting the velocity magnitude with  $v$  the velocity vector  $v$  can be written as

$$v = v_x e_x + v_y e_y = v \cos(\beta) e_x + v \sin(\beta) e_x. \quad (1)$$

The acceleration  $a = \dot{v}$  results by taking into account that the vehicle coordinate frame is a rotating frame with angular rate  $\dot{\psi}$  and this leads to

$$\begin{aligned} a &= \left( \dot{v} \cos(\beta) - v (\dot{\beta} + \dot{\psi}) \sin(\beta) \right) e_x \\ &+ \left( \dot{v} \sin(\beta) + v (\dot{\beta} + \dot{\psi}) \cos(\beta) \right) e_y \end{aligned} \quad (2)$$

Thus, the balance of forces for the x-direction is

$$F_{xfl} + F_{xfr} + F_{xrl} + F_{xrr} = m \left( \dot{v} \cos(\beta) - v (\dot{\beta} + \dot{\psi}) \sin(\beta) \right), \quad (3)$$

and for the y-direction

$$F_{yfl} + F_{yfr} + F_{yrl} + F_{yrr} = m \left( \dot{v} \sin(\beta) + v (\dot{\beta} + \dot{\psi}) \cos(\beta) \right). \quad (4)$$

Multiplying Eq. (3) with  $\cos(\beta)$  and Eq. (4) with  $\sin(\beta)$  and adding the results leads to the first differential equation of the two-track model

$$\dot{v} = \frac{1}{m} \left( \cos(\beta) \sum_i F_{xi} + \sin(\beta) \sum_i F_{yi} \right). \quad (5)$$

The second differential equation of the two-track model results from introducing Eq. (5) in Eq. (4)

$$\dot{\beta} = \frac{1}{mv} \left( \cos(\beta) \sum_i F_{yi} - \sin(\beta) \sum_i F_{xi} \right) - \dot{\psi}. \quad (6)$$

The third and last differential equation of the two-track model results from the balance of moments

$$\sum_i \mathbf{r}_i \times \mathbf{F}_i = I_z \dot{\omega}, \quad (7)$$

where  $\mathbf{r}_i$  is the lever arm for the force  $\mathbf{F}_i$  with respect to  $C$ ,  $I_z$  is the yaw moment of inertia and  $\dot{\omega} = [0, 0, \dot{\psi}]^T$ . The differential equation is

$$\begin{aligned} \ddot{\psi} &= \frac{1}{I_z} \left( \ell_f (F_{yfl} + F_{yfr}) + \frac{w}{2} (F_{xfr} - F_{xfl}) \right. \\ &\quad \left. - \ell_r ((F_{yrl} + F_{yrr}) + \frac{w}{2} (F_{xrr} - F_{xrl})) \right). \end{aligned} \quad (8)$$

In order to generate motion predictions for a 4-wheel car, suitable input quantities are needed whose effects on the forces  $F_{xi}$  and  $F_{yi}$  can easily be modelled. Using such input quantities that model the forces on each wheel, numerical integration of Eqs. (5), (6), and (8) leads to the quantities  $\dot{\psi}$ ,  $\beta$ ,  $v$  and by further integration and coordinate transformation to the position  $X$  and  $Y$  of the center of gravity  $C$  and to the yaw-angle  $\psi$  in the global coordinate frame. This way the planar location and orientation of the vehicle can be computed as a result of the chosen input quantities. Simple and intuitive input quantities that can be used to model the forces on each wheel are the steering-wheel angle and the position of the gas pedal and of the braking pedal. To use these inputs a decomposition of the forces  $F_{xi}$  and  $F_{yi}$  in the local coordinate frame of the  $i$ -th wheel is introduced, since the dependence of these forces on the longitudinal and side slip can be described mathematically. This nonlinear dependence is modelled by the “magic tire formula” that is presented in [20]. The longitudinal slip can be modelled to be a function of the gas pedal and of the brake pedal positions. The side slip can be modelled to be a function of the steering-wheel angle [21]. Thus, the planar location and orientation of the vehicle can be predicted based on hypotheses about the steering-wheel angle and brake and gas pedal positions. Such a driver model for predictions in traffic scenarios is implemented for this work and each hypothesis of the driver inputs leads to a predicted trajectory.

2) *Single-Track Model*: The single-track model is a simplification of the two-track model which results from the assumptions that the vehicle width  $w = 0$  and the slip-angle  $\beta$  is small [22]. This model can be used to describe the dynamics of cars for low values of the lateral acceleration. In this work it will be used to make predictions for bicycles in traffic scenarios. The input quantities that are used in this work for the generation of trajectories using the bicycle-model are the longitudinal acceleration and the steering angle.

By variations of input quantities mentioned above, it is possible to generate multiple hypotheses starting from an initial state of a traffic participant. The next section deals with the model used in this work to generate multiple hypotheses.

### B. Prediction and Generation of Hypothesis

The aim for introducing multiple hypotheses is to generate a detailed model of the uncertainty related to the future behavior of traffic participants.

The prediction hypotheses are categorized into two viz. the *main hypothesis* (MH) which describes a possible main maneuver, e.g., follow lane, drive straight, turn left, turn right, change lane, etc. and the *sub hypothesis* (SH) which includes the dynamic uncertainties during the execution of a certain main hypothesis, e.g., lateral and longitudinal deviation. A *main hypothesis* does not consider any abnormal driver behavior, e.g., moving out of the road. Fig. 2 shows a scenario with 3 main hypotheses such as follow lane (blue), change lane (green) and turn right (red) and a large number of *sub hypotheses* per *main hypothesis*.

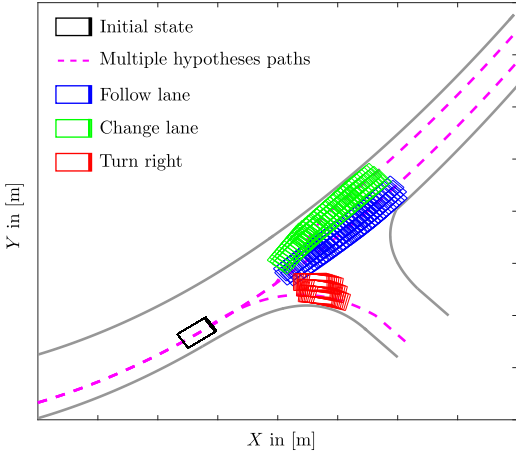


Fig. 2. Multiple Hypothesis

1) *Main Hypothesis*: The main hypotheses for the vehicle  $V_\ell$  are modelled as a discrete random variable  $h_{V_\ell}^{(MH)}$  with the outcomes {follow lane, drive straight, change lane, turn right, turn left, ...}. In this work the assignment of the probability for  $h_{V_\ell}^{(MH)}$  is rule-based and relies on expert knowledge. This assignment takes into account the current state vectors of all  $L$  traffic participants and information about the road infrastructure and traffic rules. Hereby, the state vector of the  $\ell$ -th vehicle

$$\mathbf{x}_{V_\ell} = [X_\ell, Y_\ell, v_\ell, \psi_\ell, a_{x,\ell}, a_{y,\ell}]^T \quad (9)$$

comprises the  $X_\ell$  and  $Y_\ell$  positions of the center of gravity  $C$  in the global coordinate frame, velocity  $v_\ell$ , orientation  $\psi_\ell$ , longitudinal  $a_{x,\ell}$  and lateral  $a_{y,\ell}$  acceleration of the vehicle. For example in the scenario considered in Fig. 2, it is more likely that the vehicle would make a right turn when it decelerates or has a lower velocity and it is more likely to follow the lane when the vehicle is neither accelerating nor decelerating.

At every time instance of the prediction horizon the sum of the  $M$  *main hypothesis* that are modelled for the vehicle  $V_\ell$ , should be equal to 1

$$\sum_{m=1}^M \text{P} \left( h_{V_\ell}^{(MH)} = h_{V_\ell,m}^{(MH)} \right) = 1, \quad (10)$$

where  $h_{V_\ell,m}^{(MH)}$  is the  $m$ -th possible outcome of  $h_{V_\ell}^{(MH)}$ .

2) *Sub Hypothesis*: Each of the *main hypotheses* will branch into multiple *sub hypotheses*. At the prediction time instance  $t_{\text{pred}}$ , *sub hypotheses* corresponding to the main hypothesis  $h_{V_\ell,t_{\text{pred}}}^{(MH)}$  are modelled as a multivariate random variable  $\mathbf{h}_{V_\ell,t_{\text{pred}}}^{(SH/m)}$  to include the uncertainties of the future driver behavior concerning the longitudinal and lateral dynamics. The random variable  $\mathbf{h}_{V_\ell,t_{\text{pred}}}^{(SH/m)}$  consists of two elements

$$\mathbf{h}_{V_\ell,t_{\text{pred}}}^{(SH/m)} = \begin{bmatrix} d_{V_\ell,t_{\text{pred}},\text{lon}}^{(SH/m)} \\ d_{V_\ell,t_{\text{pred}},\text{lat}}^{(SH/m)} \end{bmatrix}. \quad (11)$$

The first element of  $\mathbf{h}_{V_\ell,t_{\text{pred}}}^{(SH/m)}$  is the deviation in longitudinal direction of the vehicle  $V_\ell$  at time instance  $t_{\text{pred}}$  from its

location according to the corresponding main hypothesis  $m$  at the same prediction instance  $t_{\text{pred}}$ . The second element of  $\mathbf{h}_{V_\ell, t_{\text{pred}}}^{(SH/m)}$  is defined equivalently for the lateral deviation.

To take into account that large deviations are unlikely, the conditional probability  $p(d_{V_\ell, t_{\text{pred}}, \text{lon}}^{(SH/m)} | h_{V_\ell, m}^{(MH)})$  is modelled as a triangular *probability density function* (pdf). The bounds of the triangular pdf for the longitudinal deviation are functions of the prediction time, the velocity and the acceleration of the vehicle. The lower bound of the longitudinal deviation will be attained at the maximum deceleration  $a_{\text{decel,max}}$  of the traffic object. Similarly, the upper bound will be attained with the maximum acceleration limit of the traffic object  $a_{\text{accel,max}}$ . Equivalently, the conditional probability  $p(d_{V_\ell, t_{\text{pred}}, \text{lat}}^{(SH/m)} | h_{V_\ell, m}^{(MH)})$  is modelled as a triangular distribution considering that large deviations are less likely. The bounds of this pdf are functions of the prediction time, the road limits, the velocity and the lateral acceleration. The maximum magnitude for the lateral acceleration is denoted with  $a_{\text{lat,max}}$ .

A sub-hypothesis, i.e., a driving maneuver branching from the  $m$ -th main hypothesis, is a realization of the joint conditional pdf  $p(d_{V_\ell, t_{\text{pred}}, \text{lon}}^{(SH/m)}, d_{V_\ell, t_{\text{pred}}, \text{lat}}^{(SH/m)} | h_{V_\ell, m}^{(MH)})$  which can be decomposed assuming statistical independence between lateral and longitudinal deviations as

$$p(d_{V_\ell, t_{\text{pred}}, \text{lon}}^{(SH/m)}, d_{V_\ell, t_{\text{pred}}, \text{lat}}^{(SH/m)} | h_{V_\ell, m}^{(MH)}) = p(d_{V_\ell, t_{\text{pred}}, \text{lon}}^{(SH/m)} | h_{V_\ell, m}^{(MH)}) \cdot p(d_{V_\ell, t_{\text{pred}}, \text{lat}}^{(SH/m)} | h_{V_\ell, m}^{(MH)}). \quad (12)$$

In order to implement the approach, a quantization of the deviations  $d_{V_\ell, t_{\text{pred}}, \text{lon}}^{(SH/m)}$  and  $d_{V_\ell, t_{\text{pred}}, \text{lat}}^{(SH/m)}$  into totally  $N$  discrete values is performed and the probability of each outcome is computed based on Eq. (12). Thus the total number of hypotheses possible for a vehicle  $V_\ell$  at time instance  $t_{\text{pred}}$  will be equal to  $S$ , which is  $M$  *main hypotheses* times  $N$  *sub hypotheses*.

This way, taking into account the *main* and *sub hypotheses*, it is possible to assign probabilities to  $S$  trajectories and to construct the  $S$  dimensional vector  $\mathbf{p}(h_{V_\ell, t_{\text{pred}}})$ . The vector holds the probabilities for all  $S$  multiple hypotheses of the traffic object  $V_\ell$  at  $t_{\text{pred}}$ .

### C. Construction of POGs

The estimation of  $\mathbf{p}(h_{V_\ell, t_{\text{pred}}})$  is followed by the generation of a probabilistic representation of the future traffic scene termed as the POG. The area belonging to a traffic scenario is divided into cells of length  $\ell_{\text{cell}}$  and width  $w_{\text{cell}}$  leading to  $I$  columns and  $J$  rows in the grid. A POG  $\mathcal{G}_{t_{\text{pred}}}$  is computed for each prediction time instance  $t_{\text{pred}}$ . For a given prediction horizon, there are  $\kappa$  POGs, one for each prediction time. Let the  $(i, j)$ -th cell of the POG at a given prediction instance  $t_{\text{pred}}$  be denoted as  $g_{t_{\text{pred}}}^{ij}$ . It is important to note that a cell of a POG can be occupied simultaneously by multiple hypotheses of multiple traffic participants at a given prediction instance. The probability of occupancy  $p(o_{t_{\text{pred}}}^{ij})$  of the cell  $g_{t_{\text{pred}}}^{ij}$  is assigned based on  $\mathbf{p}(h_{V_\ell, t_{\text{pred}}})$ . Let  $\mathbf{r}_{V_\ell, t_{\text{pred}}}^{ij} \in \{0, 1\}^S$  be a binary vector of size  $S$ . The  $s$ -th element  $r_{V_\ell, t_{\text{pred}}, s}^{ij}$  denotes

the occupancy of the  $s$ -th hypothesis of the traffic object  $V_\ell$  in the  $(i, j)$ -th cell at the instance  $t_{\text{pred}}$

$$r_{V_\ell, t_{\text{pred}}, s}^{ij} = \begin{cases} 1 & \text{if } (i, j)\text{-th cell occupied by hypothesis } s \\ & \text{of the } \ell\text{-th object at instance } t_{\text{pred}} \\ 0 & \text{if } (i, j)\text{-th cell unoccupied by hypothesis } s \\ & \text{of the } \ell\text{-th object at instance } t_{\text{pred}}. \end{cases}$$

The probability of occupancy of the  $(i, j)$ -th cell in  $\mathcal{G}_{t_{\text{pred}}}$  with  $L$  traffic participants is given by

$$p(o_{t_{\text{pred}}}^{ij}) = \min \left( 1, \sum_{\ell=1}^L \left( \left( \mathbf{r}_{V_\ell, t_{\text{pred}}}^{ij} \right)^T \mathbf{p}(h_{V_\ell, t_{\text{pred}}}) \right) \right). \quad (13)$$

The min-operator in Eq. (13) is necessary since more objects can move into the same cell, this representing a crash. The probability is assigned in a similar method to all the cells, thereby generating POG  $\mathcal{G}_{t_{\text{pred}}}$ . Fig. 3 shows the constructed POG of the scenario depicted in Fig. 2 for  $t_{\text{pred}} = 2$  s. The cells concerning the road information are depicted with the probability of occupancy 1.

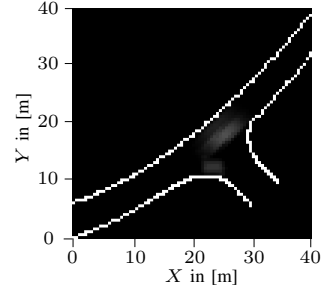


Fig. 3. Predicted-Occupancy Grid

## III. PREDICTED-OCCUPANCY GRIDS BASED ON MACHINE LEARNING

The estimation of all multiple hypotheses of traffic participants followed by the construction of POGs using the model-based approach involves a huge amount of computational effort. In order to enable real-time computation of the POGs, a machine-learning approach is adopted in this work. The goal is to perform a mapping from a suitable representation of the current state, i.e.,  $t_{\text{pred}} = 0$  s, of a traffic scenario to the  $\kappa$  POGs  $\mathcal{G}_{t_{\text{pred}}}$ . The current state representation can be constructed in vehicles from the information provided by exteroceptive and inertial sensors. The following subsection deals with the generation of a suitable current state representation for the machine-learning approach.

### A. Augmented Occupancy Grids

In this work a current state representation is proposed which consists of augmented cells in an occupancy grid  $\mathcal{OG}_0$ . The grid is chosen to be equal in size as the POGs but the values stored per cell are not estimated probabilities but a set of attributes which describe the traffic scenario corresponding to the cell. This representation  $\mathcal{OG}_0$  is called Augmented Occupancy Grid and the attributes per cell are: the occupancy, the velocity, the orientation, the longitudinal and lateral acceleration of the traffic object occupying it. For

example if a cell in  $\mathcal{OG}_0$  is occupied by a vehicle  $V_\ell$  moving with velocity  $v_\ell$ , orientation  $\psi_\ell$ , longitudinal acceleration  $a_{x,\ell}$  and lateral acceleration  $a_{y,\ell}$  the attributes for this cell are  $[1, v_\ell, \psi_\ell, a_{x,\ell}, a_{y,\ell}]^T$ . The information about the road limits is also incorporated with the corresponding cells having the attributes  $[1, 0, 0, 0, 0]^T$ . With this notation the goal of the machine-learning algorithm is to perform the mappings

$$\mathcal{OG}_0 \mapsto \mathcal{G}_{t_{\text{pred}}}. \quad (14)$$

### B. Estimation of POGs Using the RF Algorithm

1) *The Random Forest Algorithm*: The mapping from Eq. (14) is implemented in this work using the RF algorithm. It is one of the most powerful off-the-shelf machine learning algorithms. The RF algorithm has been introduced by Breiman in [18]. It is a randomized and aggregated version of the well-known [23] *Classification And Regression Tree* (CART) algorithm strengthened by the bagging (stands for *bootstrap aggregating*) technique. Given a set of input vectors and the corresponding targets, the idea underlying the RF algorithm is to construct a large number of simple classifiers with low bias, e. g., full grown decision trees and then to take a majority vote among the individual classifiers. It is proven in [18] that the algorithm does not overfit as more trees are added to the RF. The step of taking the majority vote reduces the variance of the RF classifier without increasing its bias compared to the bias and variance of the individual classifiers in the ensemble [25]. Thus, one obtains a classifier with low bias and low variance leading to a small generalization error. It is interesting to note that for classification the generalization error does not decompose into a sum of bias and variance as it is the case in regression, but in a fraction term containing the bias and variance, such that it is possible to reach the minimum of the generalization error by only decreasing the variance [24]. This explains why ensemble methods like AdaBoost or RF perform so well in classification.

In order to decrease the variance term it is important that the individual classifiers differ from each other, i. e., have a low correlation. To achieve this goal a randomization source is introduced in the construction of each tree. Although there are many possibilities to introduce randomness, the bagging technique is used since it allows to compute the oob-estimation of the generalization error [18]. In [26] Breiman gives empirical evidence that the oob-estimate is as accurate as using a test set of the same size as the training set.

2) *Estimation of POGs*: The probabilities for each cell in the POG are estimated in this work independently by using one RF classifier per cell in  $\mathcal{G}_{t_{\text{pred}}}$ . In order to realize the mapping from Eq. (14) and with the aim to determine the likeliness of occupancy, the probability  $p(o_{t_{\text{pred}}}^{ij})$  which has continuous values between 0 and 1 is quantized into discrete values. This quantization is explained further in Section IV-A. A pictorial representation of the algorithm can be seen in Fig. 4. The occupancy probability  $p(o_{t_{\text{pred}}}^{ij})$  is estimated by the RF classifier  $RF_{t_{\text{pred}}}^{ij}$ . The input  $\mathcal{OG}_0$  for all RF classifiers is the same. This holds for all  $\kappa$  POGs  $\mathcal{G}_{t_{\text{pred}}}$ .

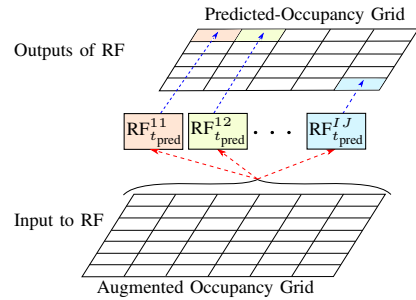


Fig. 4. Per cell prediction using Random Forest

To evaluate the ability of a set of RF classifiers to perform a mapping as shown in Fig. 4 in a first step a simplified “proof of concept” is implemented. A traffic scenario with a single vehicle driving on a road is considered. Given  $\mathcal{OG}_0$  the task of the set of RF classifiers is to predict the location of the vehicle in  $t_{\text{pred}} = 1$  s. However, multiple hypotheses dealing with the uncertainties of the driver behavior are not considered for this proof of concept, leading to target values of 0 or 1. The generated training data set comprises 300 traffic scenarios. The outputs for a test scenario and the ground truth computed by the model-based approach can be seen in the Fig. 5. The Augmented Occupancy Grid  $\mathcal{OG}_0$  consists of the road limits, the middle lane marking and a vehicle which whose center of gravity is located at the position (2.5 m, 0 m). The results of this proof of concept show the ability of a classification system as presented in Fig. 4 to implement the mapping from Eq. (14).

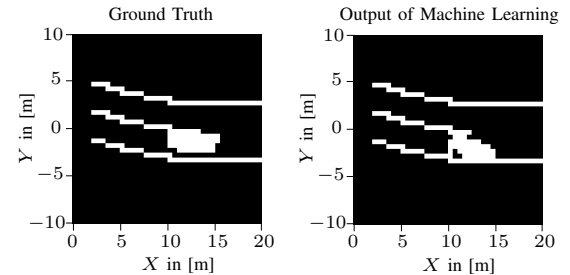


Fig. 5. Proof of concept

## IV. EVALUATION OF THE MACHINE LEARNING APPROACH

This section explains the generation of data for training and testing the machine-learning approach followed by the simulation results with their corresponding quality assessment.

### A. Generation of Data

The input and the target of the training set for the machine learning algorithm is generated using the methods explained in Subsection III-A and Section II, respectively. A complex traffic scenario with an intersection on a curved road and with 3 traffic participants (2 vehicles and 1 bicycle) on a span of  $40 \times 40$  meters is considered. The traffic scene is visualized in Fig. 6. Parameters used for the generation of the data are:  $\ell_{\text{cell}} = w_{\text{cell}} = 0.5$  m,  $a_{\text{decel,max}} = 9$  m/s<sup>2</sup>,  $a_{\text{accel,max}} =$

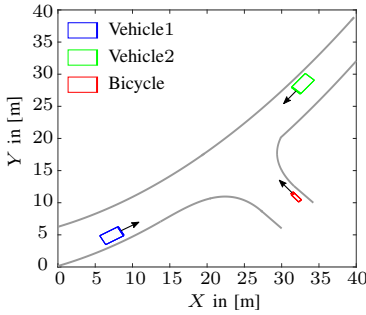


Fig. 6. Scenario under consideration

4.5 m/s<sup>2</sup>, and  $a_{\text{lat,max}} = 7 \text{ m/s}^2$ . Thus, a POG  $\mathcal{G}_{t_{\text{pred}}}$  has  $80 \times 80$  cells and leads to a total number of 6400 RF classifiers.

A number of 972 initial traffic scenarios represented by 972 Augmented Occupancy Grids  $\mathcal{OG}_0$  are generated by varying the parameters of the traffic participants such as their position, velocity and acceleration. The position for vehicles has been varied over a range of 10 m, the velocity over a range of 20 km/h and the longitudinal acceleration over 2.5 m/s<sup>2</sup>. The position for the bicycle has been varied over a range of 6 m, the velocity over a range of 10 km/h and the longitudinal acceleration over 1 m/s<sup>2</sup>.

The target data, i. e., the POGs  $\mathcal{G}_{t_{\text{pred}}}$  are obtained using the model-based approach from Subsection II-C. The prediction horizon is set to be 2 s and is represented by  $\kappa = 3$  POGs  $\mathcal{G}_{t_{\text{pred}}}$ , with  $t_{\text{pred}}$  being 0.5 s, 1.0 s and 2.0 s.

As mentioned in Subsection III-B the continuous values  $p(o_{t_{\text{pred}}}^{ij})$  must be quantized in order to estimate the likeliness of occupancy. The quantized probability value is denoted as  $p_q(o_{t_{\text{pred}}}^{ij})$ . The quantization strategy adopted in this work is

$$p_q(o_{t_{\text{pred}}}^{ij}) \in \{0, 0.25, 0.5, 0.75, 1.0\}. \quad (15)$$

These quantization values represent the degree of likeliness of occupancy. For example, 0.25 would represent less likeliness and 0.75 would state that it is more likely for the corresponding cell to be occupied.

As mentioned above the number of traffic scenarios is 972. Two-thirds of the scenarios are used for training and the remaining is used as a validation set. With  $\kappa = 3$  the prediction for 0.5 s, 1.0 s and 2.0 s leads to  $3 \times 6400$  RF classifiers, each having 700 training scenarios.

### B. Quality Assessment

It is important to quantify the quality of the machine-learning approach adopted for determining the probabilities of POG. With the oob-estimate of one RF classifier as introduced in Subsection III-B, the quality assessment can only be computed per cell of the POG. Since it is necessary to find the overall quality of the POG estimate  $\hat{\mathcal{G}}_{t_{\text{pred}}}$  computed using the machine-learning approach, a new quality quantity is formulated. Considering the fact that most of the cells in a POG have an occupancy probability of 0, such as regions outside the roads, it is useful to define region of interest while estimating the quality of prediction. Thus, only the non-zero cells are considered for the quality assessment. Let  $\mathcal{B}$  denote the set of cells with a non-zero value in the estimated

POG  $\hat{\mathcal{G}}_{t_{\text{pred}}}$  based on the machine-learning approach. Let  $\mathcal{D}$  denote the set of cells with a non-zero value in the corresponding ground truth POG  $\mathcal{G}_{t_{\text{pred}}}$  from the model-based approach. With  $K$  representing the cardinality of the set  $(\mathcal{B} \cup \mathcal{D}) \setminus (\mathcal{B} \cap \mathcal{D})$ ,

$$K = |(\mathcal{B} \cup \mathcal{D}) \setminus (\mathcal{B} \cap \mathcal{D})|, \quad (16)$$

the quality measure is defined as

$$\epsilon_{t_{\text{pred}}} = \sqrt{\frac{1}{K} \sum_{i=1}^I \sum_{j=1}^J \left( \hat{p}(o_{t_{\text{pred}}}^{ij}) - p_q(o_{t_{\text{pred}}}^{ij}) \right)^2}, \quad (17)$$

where  $\hat{p}(o_{t_{\text{pred}}}^{ij})$  is the estimated value of the  $(i, j)$ -th cell from the machine-learning approach and  $p_q(o_{t_{\text{pred}}}^{ij})$  is the quantized true occupancy probability of  $(i, j)$ -th cell from the model-based approach.

### C. Simulation Results

The simulation results for prediction time instances  $t_{\text{pred}}$  of 0.5 s, 1.0 s and 2.0 s are presented here. The histograms of non-zero  $p_q(o_{t_{\text{pred}}}^{ij})$  for  $t_{\text{pred}}$  of 0.5 s, 1.0 s and 2.0 s over the 272 test scenarios are shown in the Fig. 7. It can be seen that the number of cells taking lower values of  $p_q(o_{t_{\text{pred}}}^{ij})$  increases as  $t_{\text{pred}}$  increases. This reflects the fact that the uncertainties regarding the traffic objects increase with an increase in the prediction horizon.

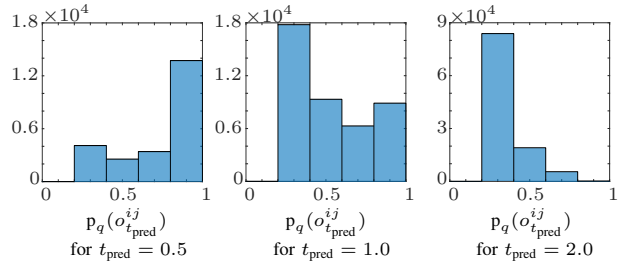


Fig. 7. Histograms of  $p_q(o_{t_{\text{pred}}}^{ij})$  for varying  $t_{\text{pred}}$

In order to perform a detailed quality assessment, error estimates according to Eq. (17) for low, middle and high values of  $p_q(o_{t_{\text{pred}}}^{ij})$  are computed, leading to the three values  $\epsilon_{t_{\text{pred}},\text{low}}$ ,  $\epsilon_{t_{\text{pred}},\text{med}}$  and  $\epsilon_{t_{\text{pred}},\text{high}}$  for each  $t_{\text{pred}}$ . The occupancy probability value corresponding to  $\epsilon_{t_{\text{pred}},\text{low}}$  is  $p_q(o_{t_{\text{pred}}}^{ij}) = 0.25$ . The occupancy probability values corresponding to  $\epsilon_{t_{\text{pred}},\text{med}}$  are  $p_q(o_{t_{\text{pred}}}^{ij}) = 0.5$  and  $p_q(o_{t_{\text{pred}}}^{ij}) = 0.75$ . The occupancy probability value corresponding to  $\epsilon_{t_{\text{pred}},\text{high}}$  is  $p_q(o_{t_{\text{pred}}}^{ij}) = 1.0$ .

The estimated mean errors  $\bar{\epsilon}_{t_{\text{pred}},\text{low}}$ ,  $\bar{\epsilon}_{t_{\text{pred}},\text{med}}$  and  $\bar{\epsilon}_{t_{\text{pred}},\text{high}}$  over all the test scenarios for varying  $t_{\text{pred}}$  are presented in Table I. The corresponding histograms are visualized in Fig. 8, Fig. 9 and Fig. 10. As it can be seen the main outcome can be stated as: low occupancy probabilities are predicted by the machine learning approach as low probabilities, middle-valued occupancy probabilities are predicted as middle-valued probabilities and high occupancy probabilities are predicted as high probabilities, independently of the prediction horizon. The machine learning approach tends to overestimate low occupancy probabilities with  $\approx 10\%$  but

TABLE I  
COMPARISON OF THE ERRORS FOR VARYING PREDICTION TIMES

	$t_{\text{pred}} = 0.5$	$t_{\text{pred}} = 1.0$	$t_{\text{pred}} = 2.0$
$\bar{\epsilon}_{t_{\text{pred}}, \text{low}}$	0.1090	0.1365	0.0930
$\bar{\epsilon}_{t_{\text{pred}}, \text{med}}$	0.2937	0.3653	0.3488
$\bar{\epsilon}_{t_{\text{pred}}, \text{high}}$	0.2315	0.3171	0.1071

the estimates never reach high occupancy probabilities. For high occupancy probabilities the machine-learning approach underestimates the occupancy probability with  $\approx 10 - 30\%$  depending on the prediction horizon, but only in a single scenario for  $t_{\text{pred}} = 2.0$  s the estimate is associated to an occupancy probability of zero. However, it must be taken into account that an occupancy probability of 1 is very unlikely for  $t_{\text{pred}} = 2.0$  s as presented in Fig. 7.

It is important to note that the quality measure defined in this work by Eq. (17) does not take into account all those cells where the classifier correctly estimates the value of  $p_q(o_{t_{\text{pred}}}^{ij}) = 0$ . However, the correct prediction of  $p_q(o_{t_{\text{pred}}}^{ij}) = 0$  is also a significant part of the classification task. For example, the mean error per cell for the POG  $\mathcal{G}_{t_{\text{pred}}}$  shown in the Fig. 11 is 0.0024, whereas  $\epsilon_{t_{\text{pred}}}$  has the value 0.1094. So, the quality assessment defined in this work does not reward the correct prediction of free space, thus leading to larger values than the mean error per cell.

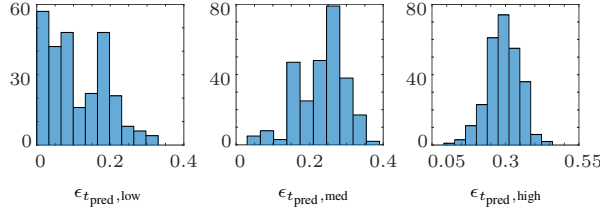


Fig. 8. Histograms of  $\epsilon_{t_{\text{pred}}}$  for  $t_{\text{pred}} = 0.5$

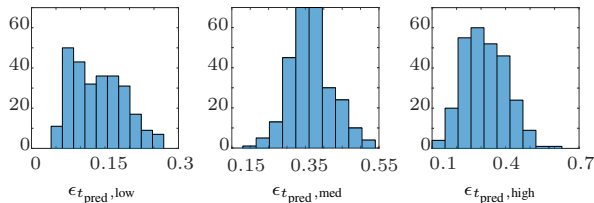


Fig. 9. Histograms of  $\epsilon_{t_{\text{pred}}}$  for  $t_{\text{pred}} = 1.0$

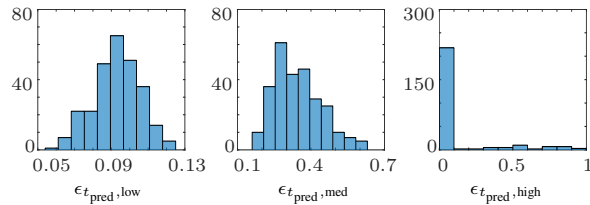


Fig. 10. Histograms of  $\epsilon_{t_{\text{pred}}}$  for  $t_{\text{pred}} = 2.0$

A key benefit of this work can be visualized exemplarily using Fig. 11. It shows the quantized values of a POG  $\mathcal{G}_{t_{\text{pred}}}$  and the corresponding machine-learning estimate  $\hat{\mathcal{G}}_{t_{\text{pred}}}$  for  $t_{\text{pred}} = 2.0$  s. The initial state of the corresponding traffic

scenario is shown in the Fig. 6. As it can be seen, the machine learning approach is able to generate good estimates of POGs. The main advantage of using the machine learning approach is that the estimate  $\hat{\mathcal{G}}_{t_{\text{pred}}}$  can be generated with relatively low computational effort as soon as the set of trained RF classifiers already exists. The computational effort for generating  $\mathcal{G}_{t_{\text{pred}}}$  using the model-based approach is huge and can only be done offline. Measurements in Matlab show that the computational time of the machine-learning approach is approx. 5 times faster than the model-based approach. Taking into account that the presented machine learning approach is highly parallelizable a real-time computation, for example on GPUs, is realistic.

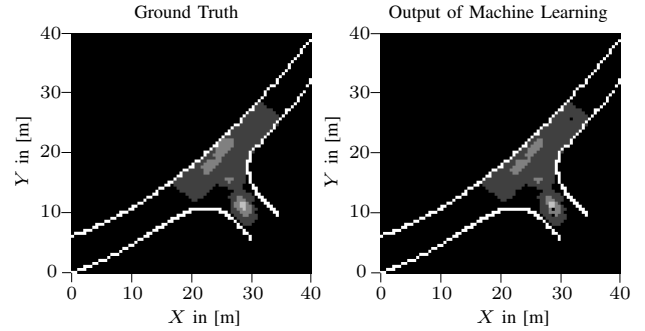


Fig. 11. Comparison between ground truth and estimated Predicted-Occupancy Grid for  $t_{\text{pred}} = 2.0$  s

## V. APPLICATIONS IN VEHICLE SAFETY

The computation of POGs in real time, for example using the machine learning approach, would enable the improvement of numerous applications in the field of vehicle safety. Some of them are presented in the following.

### A. Trajectory Planning

Vehicle safety systems that are performing autonomous interventions in the vehicle dynamics, in order to avoid a collision or to mitigate the outcome of a collision, have to plan a desired trajectory and then to control the vehicle according to this trajectory. The planning of trajectories is a challenging task and current approaches to solve this problem in real-time rely on probabilistic sampling methods like the Rapidly-exploring Random Tree (RRT) algorithm [27]. An extension of the RRT called Augmented-Closed-Loop-RRT is introduced in [28] for applications with multiple dynamic objects in complex traffic scenarios. The latter algorithm takes into account where objects will be located in future time instances in order to find collision-free trajectories. POGs that consider multiple hypotheses of objects can be used to improve this algorithm by searching for trajectories with a very low risk of collision. This can be realized by choosing trajectories which pass only through POG cells with very low probability of being occupied by other objects. Since the POGs can be implemented efficiently using the machine learning approach, the entire algorithm will maintain its fast computational speed.

### B. Criticality Estimation

POGs can also be used to estimate the risk of traffic scenarios. A survey on risk-quantities for road traffic is presented in [29]. A novel and natural way to describe the risk of a traffic scenario can be introduced using POGs. Considering a prediction time horizon of  $t_{\text{pred}}$  and  $\kappa$  POGs  $\mathcal{G}_{t_{\text{pred}}}$ , also a number of  $\kappa$  criticality-values  $c_{t_{\text{pred}}}$  can be computed, one for each prediction time. If the  $(i, j)$ -th cell in the POG  $\mathcal{G}_{t_{\text{pred}}}$  is denoted with  $g_{t_{\text{pred}}}^{ij}$  then the criticality  $c_{t_{\text{pred}}}^{ij}$  can be obtained by estimating in a first step the probability of  $g_{t_{\text{pred}}}^{ij}$  being occupied by another object than the EGO-vehicle, which is the vehicle in which the safety systems operate. Using a POG based on machine-learning as presented above, this value can be computed directly with a set of RF classifiers. Then the probability of the cell being occupied by the EGO-vehicle can be computed again using the set of RF classifiers. With these two estimated probabilities the criticality  $c_{t_{\text{pred}}}^{ij}$  for the  $(i, j)$ -th cell can be obtained by multiplying them, assuming statistical independence. The criticality  $c_{t_{\text{pred}}}$  for the prediction time instance  $t_{\text{pred}}$  can be defined to be the maximum among the criticality values in the cells

$$c_{t_{\text{pred}}} = \max_{i,j} \{c_{t_{\text{pred}}}^{ij}\}. \quad (18)$$

The criticality  $c_{\text{total}}$  of the scenario can be defined to be the maximum among the  $\kappa$  values  $c_{t_{\text{pred}}}$ . Such a criticality measure can be used in vehicle safety systems to trigger the activation of actuators.

### C. Clustering of Scenarios for Testing

The testing of vehicle safety systems is a crucial and costly task in the development process. An important aspect in the testing procedure is the choice of the test-scenarios. They must be chosen to show that the system has a very high true-positive rate and a very low false-positive rate. It depends on the system under consideration which test-scenarios are best suited to estimate these rates accurately. But a common goal for the testing of all systems is the reduction of the number of tests to a representative set. One approach to achieve this reduction is to use clustering techniques. POGs offer the possibility to cluster scenarios by taking into account also hypotheses about the future development of a traffic scenario. Then, one cluster could be represented by a single Augmented Occupancy Grid  $\mathcal{OG}_0$ .

## VI. CONCLUSIONS AND FUTURE WORK

This paper presents novel methods for the representation of the current traffic scenario and for the prediction of the future traffic scenario using occupancy grids. The prediction and its representation takes into account the uncertainties regarding the motion of traffic participants. A model-based approach and a machine learning approach using the Random Forest classifier are introduced for the prediction task. Using simulations, it is shown that the machine learning approach is able to estimate the future traffic scenario well. With trained classifiers, the computational effort to perform predictions is much smaller than using the model-based approach. This

could enable the real-time computation of Predicted Occupancy Grids.

Future work will focus on training a set of Random Forest classifiers for scenarios with varying number of objects and varying road infrastructures. Additionally, Predicted Occupancy Grids will be included in vehicle safety algorithms for trajectory planning and criticality estimation.

## REFERENCES

- [1] N. Kaempchen, B. Schiele, and K. Dietmayer, Situation assessment of an autonomous emergency brake for arbitrary vehicle-to-vehicle collision scenarios, *IEEE Trans. Intell. Transp. Syst.*, Dec 2009.
- [2] S. Herrmann, W. Utschick, M. Botsch and F. Keck, Supervised Learning via Optimal Control Labeling for Criticality Classification in Vehicle Active Safety, *IEEE International Conference on Intelligent Transportation Systems*, 2015.
- [3] C. Hermes, C. Wöhler, K. Schenk *et al.*, Long-Term Vehicle Motion Prediction, *Proc. of the IEEE Intelligent Vehicles Symposium*, 2009.
- [4] D. Vasquez and T. Fraichard, Motion Prediction for Moving Objects: A Statistical Approach, *Proc. of the IEEE International Conference on Robotics and Automation*, 2004.
- [5] A. Broadhurst, S. Baker and T. Kanade, Monte Carlo Road Safety Reasoning, *Proc. of the IEEE Intelligent Vehicles Symposium*, 2005.
- [6] T. Hülnhagen, I. Dengler, A. Tamke *et al.*, Maneuver Recognition Using Probabilistic Finite-State Machines and Fuzzy Logic, *Proceedings of the IEEE Intelligent Vehicles Symposium*, 2010.
- [7] D. Kasper, G. Weidl, T. Dang *et al.*, Object-Oriented Bayesian Network for Detection of Lane Change Maneuvers, *IEEE Intelligent Transportation Systems Magazine*, 2012.
- [8] I. Dagli, M. Brost and G. Breuel, Action Recognition and Prediction for Driver Assistance Systems Using Dynamic Belief Networks, *Lecture Notes in Computer Science*, 2003.
- [9] D. Meyer-Delius, C. Plagemann and W. Burgard, Probabilistic Situation Recognition for Vehicular Traffic Scenes, *Proceedings of the IEEE International Conference on Robotics and Automation*, 2009.
- [10] M. Schreier, V. Willert and J. Adamy, Bayesian, Maneuver-Based, Long-Term Trajectory Prediction and Criticality Assessment for Driver Assistance Systems, *IEEE International Conference on Intelligent Transportation Systems*, 2014.
- [11] T. Gindel, S. Brechtel and R. Dillmann, A probabilistic model for estimating driver behaviors and vehicle trajectories in traffic environment, *IEEE International Conf. on Intell. Transp. Systems*, 2010.
- [12] S. Lefèvre, C. Laugier and J. Ibanez-Guzman, Risk assessment at road intersections: Comparing intention and expectation, *IEEE Intelligent Vehicles Symposium*, 2012.
- [13] S. Thrun, W. Burgard and D. Fox, *Probabilistic Robotics*, MIT Press, 2005.
- [14] P. Stepan, M. Kulich and L. Preucil, Robust data fusion with occupancy grid, *IEEE Trans. on Systems, Man and Cybernetics*, 2005.
- [15] M. Himmelsbach, F. Hundelshausen, H. Wünsche, LIDAR-Based Perception for Offroad Navigation, *Proceedings of FAS*, 2008.
- [16] B. Siciliano and O. Khatib, *Handbook of Robotics*, Springer, 2008.
- [17] C. Chen, C. Tay, C. Laugier and K. Mekhnacha, Dynamic environment modeling with gridmap: A multiple-object tracking application, *International Conf. on Control, Automation, Robotics and Vision*, 2006.
- [18] L. Breiman, E. Schapire, Random Forests, *Machine Learning*, 2001.
- [19] R. Schubert, E. Richter and G. Wanielik, Comparison and evaluation of advanced motion models for vehicle tracking, *11th International Conference on Information Fusion*, 2008.
- [20] E. Bakker, L. Nyborg and H. B. Pacejka, Tyre modelling for use in vehicle dynamics studies, *Society of Automotive Engineers international congress and expo*, 1987.
- [21] G. Baffet, A. Charara, D. Lechner, Estimation of tire-road forces and vehicle sideslip angle, *Advances in Robotics, Automation and Control*, 2008.
- [22] R. N. Jazar, *Vehicle Dynamics: Theory and Application*, Springer, 2009.
- [23] L. Breiman, J. H. Friedman, R. A. Olshen and C. J. Stone, *Classification and Regression Trees*, Wadsworth, 1984.
- [24] J. H. Friedman, On bias, variance, 0/1-loss and the curse of dimensionality, *Data Mining and Knowledge Discovery*, 1997.
- [25] P. Geurts, D. Ernst and L. Wehenkel, *Extremely randomized trees*, *Machine Learning*, 2006.

- [26] L. Breiman, Out-of-bag Estimation, Statistics at UC Berkeley, 1996.
- [27] S. M. LaValle, Rapidly-exploring random trees: A new tool for path planning, Technical Report, Computer Science Department Iowa State University, 1998.
- [28] A. Chaulwar and M. Botsch, Planning of safe trajectories in dynamic multi-object traffic-scenarios, Traffic and Logistics Engineering, 2016.
- [29] S. Lefevre, D. Vasquez, and C. Laugier, A survey on motion prediction and risk assessment for intelligent vehicles, ROBOMECH, 2014.